Toxicology in Vitro xxx (2013) xxx–xxx

Contents lists available at ScienceDirect

Toxicology in Vitro

journal homepage: www.elsevier.com/locate/toxinvit

Transferrin as a drug carrier: Cytotoxicity, cellular uptake and transport kinetics of doxorubicin transferrin conjugate in the human leukemia cells

Marzena Szwed [a,*], Agnieszka Matusiak [b], Audrey Laroche-Clary [c], Jacques Robert [c], Ilona Marszalek [d], Zofia Jozwiak [a]

[a] Department of Thermobiology, Faculty of Biology and Environmental Protection, University of Lodz, Pomorska 141/143 Street, 90-236 Lodz, Poland
[b] Department of Immunology and Infectious Biology, Faculty of Biology and Environmental Protection, University of Lodz, Banacha 12/16 Street, 90-237 Lodz, Poland
[c] INSERM U916, Institut Bergonié, Université Bordeaux Segalen, 33076 Bordeaux, France
[d] Department of Biophysics, Institute of Biochemistry and Biophysics, Polish Academy of Sciences, Pawińskiego 5a, 02-106 Warsaw, Poland

ARTICLE INFO

Article history:
Received 13 April 2013
Accepted 11 September 2013
Available online xxxx

Keywords:
Doxorubicin (DOX)
Doxorubicin–transferrin conjugate (DOX–TRF)
Cytotoxicity
Leukemia cells
Intracellular drug accumulation

ABSTRACT

Leukemias are one of most common malignancies worldwide. There is a substantial need for new chemotherapeutic drugs effective against this cancer. Doxorubicin (DOX), used for treatment of leukemias and solid tumors, is poorly efficacious when it is administered systemically at conventional doses. Therefore, several strategies have been developed to reduce the side effects of this anthracycline treatment. In this study we compared the effect of DOX and doxorubicin–transferrin conjugate (DOX–TRF) on human leukemia cell lines: chronic erythromyeloblastoid leukemia (K562), sensitive and resistant (K562/DOX) to doxorubicin, and acute lymphoblastic leukemia (CCRF-CEM). Experiments were also carried out on normal cells, peripheral blood mononuclear cells (PBMC). We analyzed the chemical structure of DOX–TRF conjugate by using mass spectroscopy. The *in vitro* growth-inhibition assay XTT, indicated that DOX–TRF is more cytotoxic for leukemia cells sensitive and resistant to doxorubicin and significantly less sensitive to normal cells compared to DOX alone. During the assessment of intracellular DOX–TRF accumulation it was confirmed that the tested malignant cells were able to retain the examined conjugate for longer periods of time than normal lymphocytes. Comparison of kinetic parameters showed that the rate of DOX–TRF efflux was also slower in the tested cells than free DOX. The results presented here should contribute to the understanding of the differences in antitumor activities of the DOX–TRF conjugate and free drug.

1. Introduction

Doxorubicin (DOX) is an effective antineoplastic agent with antitumor activity against many solid tumors and leukemias but its utilization in anticancer therapy is limited by a number of factors including their low therapeutic index and the rapid emergence of drug resistant cell populations (Jungsuwadee et al., 2012; Swiech et al., 2012). The clinical use of DOX is limited, due to cumulative, dose-dependent side effects such as cardiotoxicity and myelosuppression. Consequently, many approaches have been carried out to improve the chemotherapeutic potency of doxorubicin and other anthracyclines (Luo et al., 2011; Salvatorelli et al., 2012). The goal of anticancer drug development is to identify agents that are effective cancer medicines and yet have minimal systemic side effects. A way to improve the selectivity of cancer therapy is to direct drug activity against therapeutic targets that display altered levels of expression in malignant versus normal cells (Kratz et al., 2008). The use of drug carriers, such as liposomes, dendrimers, nanoparticles, antibodies and others may be part of this approach in allowing increased intracellular concentrations of the cytotoxic agents in cancer cells, therefore helping to overcome the chemoresistance of neoplastic cells (Haag and Kratz, 2006).

Effective and selective anticancer drug carriers are protein conjugates of anthracyclines. Transferrin (TRF) is a plasma protein that can be used as a carrier of anthracyclines because receptors for this protein are overexpressed at the surface of cancer cells, due to the high demand of tumor cells for iron ions, which participate in energy production, heme synthesis, and cell proliferation (Lubgan

Abbreviations: DOX, doxorubicin; DOX–TRF, doxorubicin–transferrin conjugate; TRF, transferrin; K562, chronic erythromyeloblastoid leukemia cells; CCRF-CEM, acute lymphoblastic leukemia cells; PBMC, peripheral blood mononuclear cells; IMS, Ion Mobility Mass Spectrometry; Ω, collisional cross section; tD, drift times; k_{in}, influx rate constant; V_{in}, influx rate; $U_{t=60}$, drug taken up by cells within 60 min; k_{out}, efflux rate constant; V_{out}, efflux rate; $E_{t=60}$, drug removed by cells within 60 min.

* Corresponding author. Tel.: +48 42 635 44 81; fax: +48 42 635 44 73.
E-mail address: szwedma@biol.uni.lodz.pl (M. Szwed).

0887-2333/$ - see front matter © 2013 Published by Elsevier Ltd.
http://dx.doi.org/10.1016/j.tiv.2013.09.013

et al., 2006). Moreover, this protein is commercially available and does not produce an immune response in patients. In addition, intensive transport of transferrin to tumor cells is possible due to the increased permeability of blood tumor vessels. The diameter of the slots in the tumor capillaries range from 100 to 1200 nm, while in normal tissues it is about 100 times smaller (Nevozhay et al., 2007).

Transferrin has recently shown promise as a carrier for anticancer agents. A mitomycin–transferrin conjugate, forming cytostatic cross-links with DNA, showed a cytotoxic effect on HepG2 cells (Human hepatocellular liver carcinoma) and HL60 cells (Human promyelocytic leukemia), with inhibition of cell proliferation *in vitro* (Tanaka et al., 2001).

The purpose of our work is to analyze the effectiveness of the transport of a DOX–TRF conjugate through the cellular membrane of human leukemia cells and its intracellular distribution in comparison with free doxorubicin. It has been estimated that leukemia cells have from 150,000 to 1,000,000 TRF receptors on their surface, while normal cells are deficient in this type of receptor (Lubgan et al., 2009; Barabas et al., 1992). We have chosen two human leukemia cell lines: chronic erythromyeloblastoid leukemia cells (K562) and acute lymphoblastic leukemia cells (CCRF-CEM), which present substantial differences in oncogenesis mechanisms and drug sensitivity. Peripheral blood lymphocytes were used as normal cells for comparison.

2. Materials and methods

2.1. Chemical compounds

DOX was obtained from Sequoia Research Products (Pangbourne, United Kingdom). RPMI 1640 bicarbonate medium was supplied by Lonza (Vievres, Belgium), fetal bovine serum (FBS), penicillin and streptomycin were from Gibco (Edinburgh, Scotland). Human transferrin, glutaraldehyde and ethanolamine used for conjugation were purchased from Sigma. All other chemicals and solvents with high analytical grade were obtained from POCH S.A. (Gliwice, Poland).

Doxorubicin was coupled to TRF using the modified conjugation procedure developed by Berczi et al. (1993), Patent claim No WIPO ST 10/C PL 402896). DOX–TRF was chromatographed on a column of Sepharose CL-4B. The optical spectrum of each fraction was determined using a UV/VIS spectrophotometer (Perkin Elmer SL-5B) and the collected fractions were analyzed by sodium dodecyl sulfate–polyacrylamide gel electrophoresis (SDS–PAGE), according to Lubgan et al. (2009).

2.2. Mass spectrometry experiments – MALDI-TOF measurement

The molecular weight of doxorubicin–transferrin conjugate was determined by mass spectrometry (MS). We calculated the mass-to-charge ratio of transferrin or its conjugate with doxorubicin, and the mass spectra of tested compounds were evaluated. Mass difference allowed the determination of the molar ratio of drug conjugated to protein. Identification of the molecular weight was made using MALDI-TOF spectrometer (Bruker Co.) in a linear ion mode for positive ions detection. For this purpose, solutions of native protein (transferrin) and transferrin conjugated to doxorubicin (DOX–TRF) were prepared at a concentration 15 μg/ml. A saturated solution of matrix–sinapic acid (SA) in 50% acetonitrile and 0.05% trifluoroacetic acid was prepared. The native protein or the conjugate was mixed with the matrix solution in a volume ratio of 1:1, and 0.5 μl of the sample was applied to a steel plate.

2.3. Mass spectrometry experiments – Ion Mobility Mass Spectrometry (IMS)

In order to verify that the shape and size of transferrin did not change after attachment of doxorubicin, we compared the collisional cross section (Ω (Å^2)) of native transferrin and DOX–TRF conjugate. For this experiment we used a hybrid mass spectrometry technique combined with the separation of ions according to their collisional cross section (IMS, Ion Mobility Mass Spectrometry).

Ions generated in the electrospray source enter the ion mobility device and travel toward the detector with associated drift times (tD (ms)). The collisional cross section (Ω) value and tD are linked by the formula (Giles et al., 2004; Myung et al., 2003):

$$\frac{\Omega}{q} = atDb$$

where tD is the measured drift time (ms), Ω is the collisional cross section (Å^2), q is the molecular charge and a, b are the constants that remain unchanged and determined in a given experiment.

To determine the parameters of the equation it was necessary to measure protein standards, draw a calibration curve and measure studied samples under the same condition.

The experiment began with measurements of the drift times (tD) of standard proteins with known values of m/z and the corresponding collisional cross sections. Cytochrome c and ubiquitin were measured to draw the calibration curve (Ruotolo et al., 2008, 2007). Under the same conditions we measured the drift times for transferrin and the DOX–TRF conjugate.

The measurement was made using an ESI–TOF mass spectrometer (SYNAPT G2 HDMS Waters Co.) in positive ion mode. The spectrometer settings were: capillary voltage – 2.5 kV, sampling cone voltage – 70 V. Solutions of native transferrin and DOX–TRF conjugate were prepared at a concentration of 15 μg/ml. They were then subjected to dialysis against 5 mM ammonium acetate pH 7.4. All data acquisition and processing were carried out with MassLynx (V4.1) and DriftScope (V2.1) software supplied with the instrument.

2.4. Cell cultures

CCRF-CEM cells were received from Prof. G. Bartosz (Department of Molecular Biophysics, University of Lodz, Poland). K562 cells sensitive and resistant to doxorubicin were a kind gift from Prof. J. Robert at Institute Bergonie, Bordeaux, France. K562/DOX cells were cultured in continuous presence of 0.02 μM DOX and the cells were resistant to DOX due to overexpression of the MDR1 protein (Tsuruo et al., 1986). Peripheral blood mononuclear cells were obtained from young (23–25 years), non-smoking men. The lymphocytes were isolated by centrifugation in a density gradient of Histopaque (30 min, 300*g*, 22 °C). Cell viability, evaluated by trypan blue exclusion, was found to be about 99%. In the case of lymphocytes, each experiment was performed on cells obtained from the blood of three different donors. All cells were grown at 37 °C in a 5% CO_2 atmosphere in RPMI 1640 supplemented with 10% heat-inactivated FBS, penicillin (10 U/ml) and streptomycin (50 μg/ml).

2.5. Cell cytotoxicity assay

The cytotoxicity of DOX and DOX–TRF to human tumor and normal cells was measured in 96-well plates by a XTT (2,3-Bis (2-methoxy-4-nitro-5-sulfophenyl)-2H-tetrazolium-5-carboxanilide inner salt) colorimetric assay. This method is based on the cleavage of XTT by metabolically active cells. For this purpose, 10^4 (CCRF-CEM, K562, K562/DOX) or 10^5 (PBMC) cells were seeded in each well in 0.1 ml of culture medium. Then, 0.05 ml DOX or DOX–TRF of different concentrations were added to the appropriate wells, and cells were incubated with drugs for 72 h. At the end of incubation, the cells were centrifuged (230*g* for 10 min at 4 °C), and the medium was gently removed. At that time, 50 μl XTT at the final concentration of 0.3 mg/ml medium was added to each well and the microplates were incubated for 4 h. The plates were mechanically agitated for 1 min, and an absorbance at 450 nm was measured with a microplate reader (Awareness Technology Inc., USA). Cytotoxicity of DOX and conjugate was expressed as IC_{50}, i.e. the concentration of drug that reduces cell viability by 50% relative to the control (untreated cells).

2.6. Intracellular accumulation of DOX and DOX–TRF

Intracellular DOX or DOX–TRF accumulation was evaluated by flow cytometry (LSRII, BD Biosciences). The cells (4×10^5 in 3 ml of culture medium) were plated onto 30-mm Petri dishes and incubated at a concentration of 0.5 μM DOX or DOX–TRF for various periods: 0.5, 1; 2; 4; 6; 12 and 24 h (37 °C, 5% CO_2). After incubation, the cells were centrifuged and suspended in ice-cold PBS. The intensity of drug fluorescence was measured on a Becton–Dickinson flow cytometer using Flow Jo cytology software; 10^5 cells were counted in each sample and each experiment was repeated at least 4 times. As a control, the autofluorescence of the untreated cells was used. In addition, cells were viewed using inverted fluorescence microscopy (Olympus IX70, Japan) with a suitable filter, under 400× magnification.

2.7. Estimation of doxorubicin or doxorubicin–transferrin uptake

The amount of DOX and DOX–TRF conjugate taken up by the cells was determined using flow cytometry (LSRII, BD Biosciences). Drugs at a final concentration of 5 μM were added to 10^6cells in 1 ml of medium for periods ranging from 5 to 60 min (37 °C). DOX fluorescence was obtained using 488 nm laser excitation wavelength. Fluorescence was transmitted through FL2 channel. The parameter analyzed was the slope of the straight line, considered as the rate of drug accumulation in cells. The results are presented as a percent of control (autofluorescence of the untreated cells taken as a 100%).

2.8. Drug transport and intracellular distribution

The study of the dynamics of DOX and DOX–TRF transport through the cell membrane was carried out according to the method described by Przybylska et al. (2001). Cells were seeded into 96-well plates at a density of 8×10^4 cells per well in 0.2 ml of culture medium. The plates were then centrifuged (230*g* for 10 min at 4 °C) and 0.05 ml DOX or DOX–TRF at a concentration of 2 μM was added. The cells were incubated with drugs for 5–60 min (37 °C, 5% CO_2). An equal volume of HBSS (140 mM NaCl, 5 mM KCl, 0.8 mM $MgCl_2$, 1.8 mM $CaCl_2$, 1 mM Na_2HPO_4, 10 mM HEPES, and 1% glucose) was added to the control samples. The samples containing drug without cells were used as references for initial drug concentration. At the indicated time points, the supernatant was moved to black 96-well microtiter plates. The amount of DOX and DOX–TRF in the medium was evaluated using fluorescent multiwell plate reader *Fluoroskan Ascent FL., Labsystem Inc* (λ_{ex} = 488 nm, λ_{em} = 566 nm). The amount of drug in extracellular medium and associated with the cells was calculated from the standard curve, representing the relationship between drug concentration and fluorescence intensity.

Kinetic parameters associated with DOX and DOX–TRF transport into lymphocytes and leukemia cells were calculated as previously described (Andreoni et al., 1996). A simple model of transport kinetics was assumed. The intracellular concentration of drug (C) in steady state was taken from the equation:

$$C = M_{tot} - M_t \quad (1)$$

where M_{tot} is the total amount of drug to which cells were initially exposed and M_t is the amount of drugs in external medium at various times of incubation.

Furthermore, the initial rate of DOX and DOX–TRF uptake ($I_{t=0}$) is given as the first derivative of the curve representing time-dependence of drug transport. At the equilibration state, the uptake rate constants of drug transport were calculated according to the assumption that both DOX and conjugate influx followed a first order equation.

$$I_{t=0} = k_{in} M_{tot} \quad (2)$$

where k_{in} is the influx rate constant. Values of M_{tot} and k_{in} allowed the estimation of the quantity of drug taken up by cells (U), which was then evaluated from the rate equation transformation:

$$U = M_{tot}(1 - e_{in}^{-k \cdot t}) \quad (3)$$

Under these conditions, the kinetic parameters for drugs effluxed by cells (k_{out} and $E_t = 0$) were analyzed in the same way from the curves representing the time dependence of the values gained by the judgment of the intracellular amount of drug (C) from the amount of drug taken up by cells (U) at the same incubation time.

2.9. Statistical analysis

Data are expressed as a means ± S.D. An analysis of variance (ANOVA) with a Tukey post hoc test was used for multiple comparisons. Three-way analysis of variance was used to test DOX and DOX–TRF cytotoxicity, accumulation and uptake between cell lines. All statistics were calculated using the STATISTICA program (StatSoft, Tulsa, OK, USA). A P value of <0.05 was considered significant.

3. Results

3.1. Determination of the molecular weight of the doxorubicin–transferrin conjugate by mass spectrometry

The analysis of the mass spectrum of native transferrin and DOX–TRF conjugate (Fig. 1) allows us to determine the molecular weight of transferrin on 78.40 kDa and DOX–TRF conjugate on 79.50 kDa. Taking into account the fact that free doxorubicin has a molecular weight 543 Da, we concluded that the conjugate results from the association of two molecules of DOX and one molecule of TRF.

3.2. Ion mobility analysis of doxorubicin–transferrin conjugate

Collisional cross section is a physical quantity, which allows the comparison of the overall shape and size of the transferrin molecule before and after association to doxorubicin. Fig. 2 shows a typical spectrum for IMS measurement and shows the dependence of drift time (tD) and m/z value. Each spot on the spectrum represents a different charge state (z) which is expected for electrospray ionization. For both transferrin and conjugate there were only single values of drift times for each charge states. This profile shows that transferrin and the conjugate occur in a homogeneous structure state. Using the calibration curve, we calculated the values of collisional cross sections (Ω (Å^2)) for every charge states of transferrin and the conjugate (Table 1). Charge attachment during generation of ions causes small structure expansion leading to

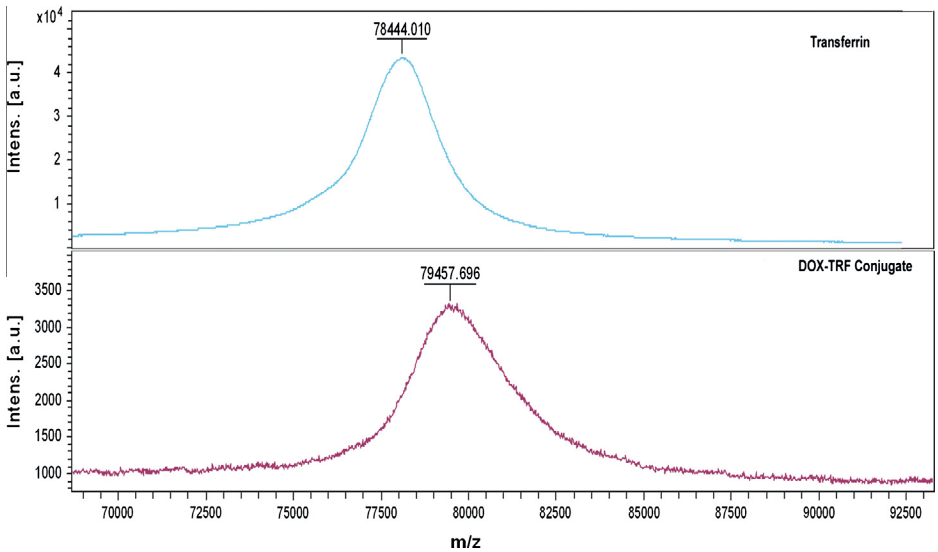

Fig. 1. Mass spectrum of free doxorubicin and doxorubicin transferrin conjugate.

increased collisional cross section, which is expected. However, Ω does not differ between transferrin and the conjugate.

Results were also compared with the theoretical value of the collisional cross section of transferrin. Theoretical calculations were performed using CCS calc (Bruker Co.) software, based on available data for transferrin in the PDB (Protein Data Bank) database. The calculated value of collisional cross section for transferrin was 4744 Å^2. This shows that theoretical and experimental values of Ω are in firm agreement.

Summarizing this experiment, the results indicate that there was no difference in collisional cross sections between free transferrin and the DOX–TRF conjugate. This indicates that the conjugation of DOX to transferrin did not change the structure of the protein.

3.3. Cytotoxicity assay

As shown in Table 2, the cells presented a significantly different sensitivity to doxorubicin and DOX–TRF. The three leukemia cell lines were consistently more sensitive to DOX–TRF than to DOX, whereas normal lymphocytes were, significantly, 2-fold less sensitive to DOX–TRF conjugate than to DOX. The conjugate appears more cytotoxic than the free drug against tumor cells and less toxic than the free drug against normal lymphocytes. In addition, DOX–TRF is much less cytotoxic against normal lymphocytes than against each of the leukemia cell lines, even the doxorubicin-resistant K562 clone.

3.4. DOX and DOX–TRF conjugate accumulation in normal and leukemia cells

To analyze whether the cytotoxic activity of DOX and DOX–TRF was related to their intracellular level, drug accumulation was estimated as a function of time (Fig. 3). Fluorescence intensity of DOX in K562, K562/DOX and CCRF-CEM cells reached a maximal level after 2 h and 4 h incubation, respectively, and drug fluorescence slowly decreased thereafter (6–24 h). By contrast, DOX–TRF fluorescence progressively increased in leukemia cell lines up to 24 h incubation. Accumulation of free DOX and DOX–TRF was higher in CCRF-CEM cells than in K562 cells (about 2 and 2.5-fold respectively); in K562/DOX cells, free drug had a markedly lower accumulation than in the parental cells, whereas DOX–TRF was similarly accumulated in both cell lines. In PBMC, DOX fluorescence was as high as in CCRF-CEM cells, whereas DOX–TRF fluorescence rapidly reached a maximum level after 1 h incubation and then gradually decreased. These findings show that there was no obvious relationship between drug accumulation and cytotoxicity since DOX–TRF was more cytotoxic to and less accumulated within leukemia cells than DOX. In addition, Pgp-related drug resistance was associated with a marked reduction in DOX accumulation but not in DOX–TRF accumulation. Finally, a different mode of accumulation of DOX–TRF and DOX operates in normal and leukemic cells.

The intracellular location of the compounds in leukemia and normal cells was evaluated by fluorescence microscopy (Fig. 4). Alterations in the structure, size and shape of the cell nucleus were detected after 12 h of treatment with both drugs. DOX–TRF was mainly located in cytoplasm. At early times of incubation, we observed a bright red fluorescence in the region of cellular membrane. In addition, free DOX was mainly accumulated in the nucleus whereas its conjugate could be gathered in other cell organelles. In PBMC, DOX and DOX–TRF, fluorescence was markedly weaker than in leukemia cells, sensitive or resistant to doxorubicin.

3.5. Flow cytometry analysis of the drugs

When studied as a function of time at the concentration of 5 μM, the accumulation of DOX and DOX–TRF conjugate in leukemia cells did not reach a plateau (Fig. 5). In contrast, a plateau was reached after short incubation times in PBMC. Additionally, the rate of influx of DOX–TRF was slower than that of DOX in leukemia cells or PBMC (Fig. 5) (11.7 units for K562, and 35.7 units for CCRF-CEM). Besides this, the difference between the rate of DOX or DOX–TRF accumulation was also observed in normal cells during the time of experiment, since the slope of the rate of accumulation equalled 7.7 units for DOX and 4.4 units for DOX–TRF, respectively. The results clearly show that DOX–TRF needs more time to reach the same level as DOX in leukemic cells.

3.6. Transport kinetics and cellular distribution

The transport of DOX and DOX–TRF through the cellular membrane was estimated indirectly from the measurement of the drug fluorescence in external medium. Our results indicate substantial

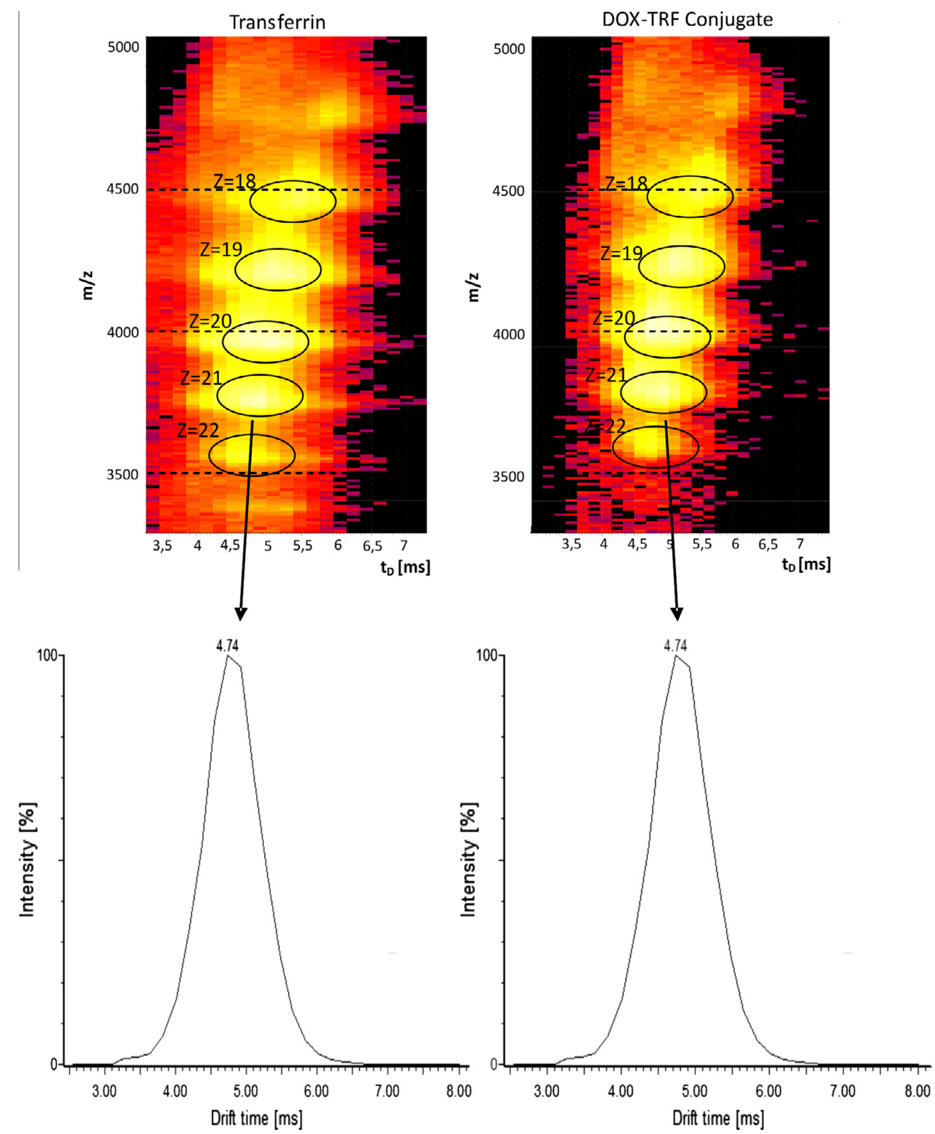

Fig. 2. The conjugate and free transferrin IMS spectrum. The upper panel shows signal series resolved in the domain of m/z (vertical axis) and drift time (t_D [ms]) shown on horizontal axis. Black ellipses mark signals of different charge states, as described. The lower profile panel shows a cross-section for $Z = 21$ charge state in the domain of drift time (t_D [ms]). The profiles are the same which concludes that collisional cross section of transferrin does not change after attachment of doxorubicin.

Table 1
Collisional cross sections (Ω [Å^2]) for every charge state (z) of transferrin and DOX–TRF conjugate.

Sample	m/z	Ω (Å^2)	z	t_D (ms)	Ω/z
Transferrin	4363	4724	18	5,29	262
	4134	4812	19	4,92	253
	3927	4880	20	4,56	244
	3740	5222	21	4,74	249
	3570	5368	22	4,56	244
DOX–TRF conjugate	4419	4724	18	5,29	262
	4186	4812	19	4,92	253
	3977	4880	20	4,56	244
	3788	5222	21	4,74	249
	3616	5368	22	4,56	244

Table 2
Cytotoxicity of free doxorubicin and doxorubicin conjugated to transferrin in PBMC. CCRF-CEM and K562 cell lines sensitive and resistant to DOX. The values are the IC_{50} mean values ± SD of 4–5 independent experiments.

Cell lines	IC_{50} values	
	DOX (nM)	DOX–TRF (nM)
CCRF-CEM	131.21 ± 14.59[#]	57.16 ± 2.81[*,#]
K562	269.61 ± 20.13[#]	72.4 ± 5.67[*,#]
K562/DOX	2572.35 ± 124.78[#]	260.97 ± 16.34[*,#]
PBMC	566.08 ± 54.66	1132.16 ± 109.25[*]

[*] Significant differences between cells treated with DOX and DOX–TRF ($p < 0.05$).
[#] Significant differences between leukemia cells and PBMC ($p < 0.05$).

differences in cellular uptake of DOX and DOX–TRF by normal and malignant cells. The curves representing the amount of drug taken up as a function of time (U) and excluded by cells during the same time (E) are presented in Fig. 6 and the kinetic parameters evaluated from them are presented in Table 3. We have shown that DOX was transported faster to cells than its conjugate in PBMC, CCRF-CEM and K562 sensitive cells, whereas DOX–TRF was transported faster than DOX in K562 resistant cells. In contrast, the rate of DOX–TRF efflux was lower than that of DOX in leukemia cells but they were similar for PBMC. The amount of DOX removed by cells during 60-min incubations was markedly lower in normal cells than in malignant cells.

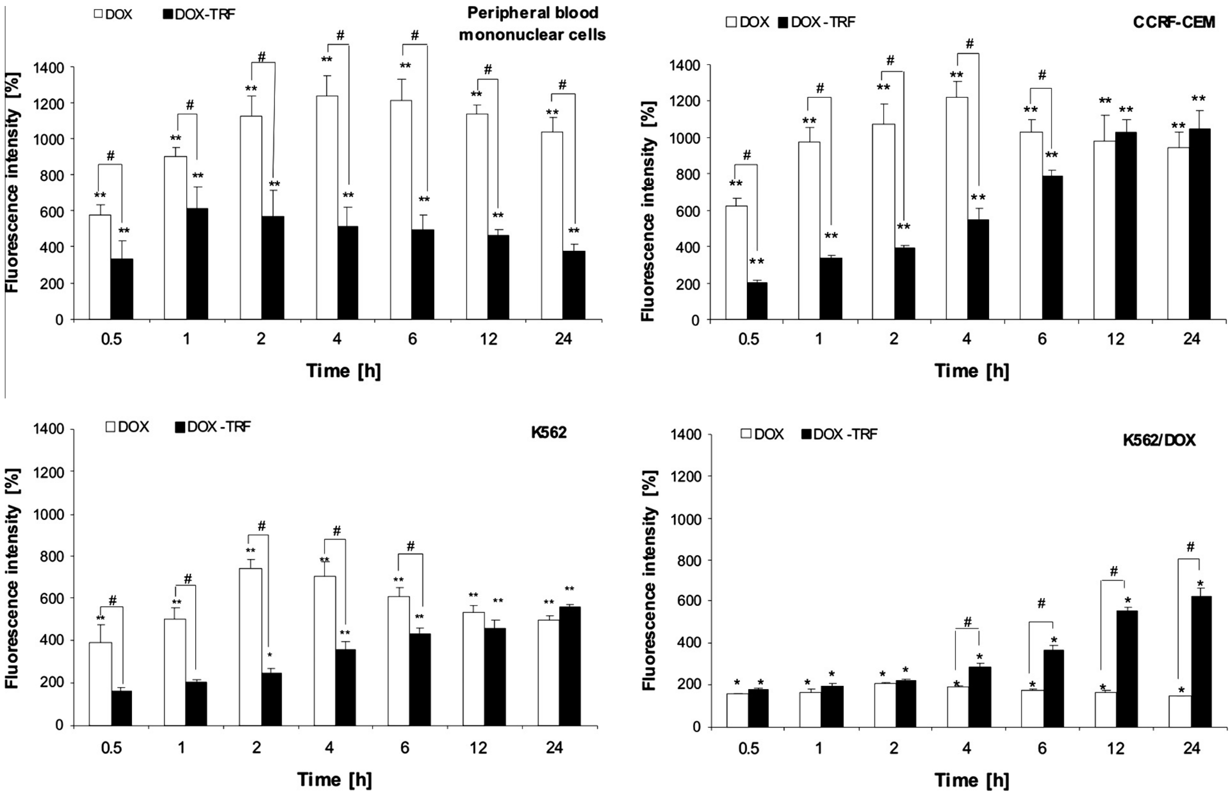

Fig. 3. DOX and DOX–TRF accumulation in PBMC, CCRF-CEM, K562 and K562/DOX cell lines. Cells were treated with 0,5 μM of both drugs for 0.5 h to 24 h. Results represent means ± SD of six independent experiments. Significant differences between treated and control cells, taken as 100%: $^{*}p < 0.05$, $^{**}p < 0.01$; significant differences between cells treated with free doxorubicin and DOX–TRF conjugate: $^{\#}p < 0.05$.

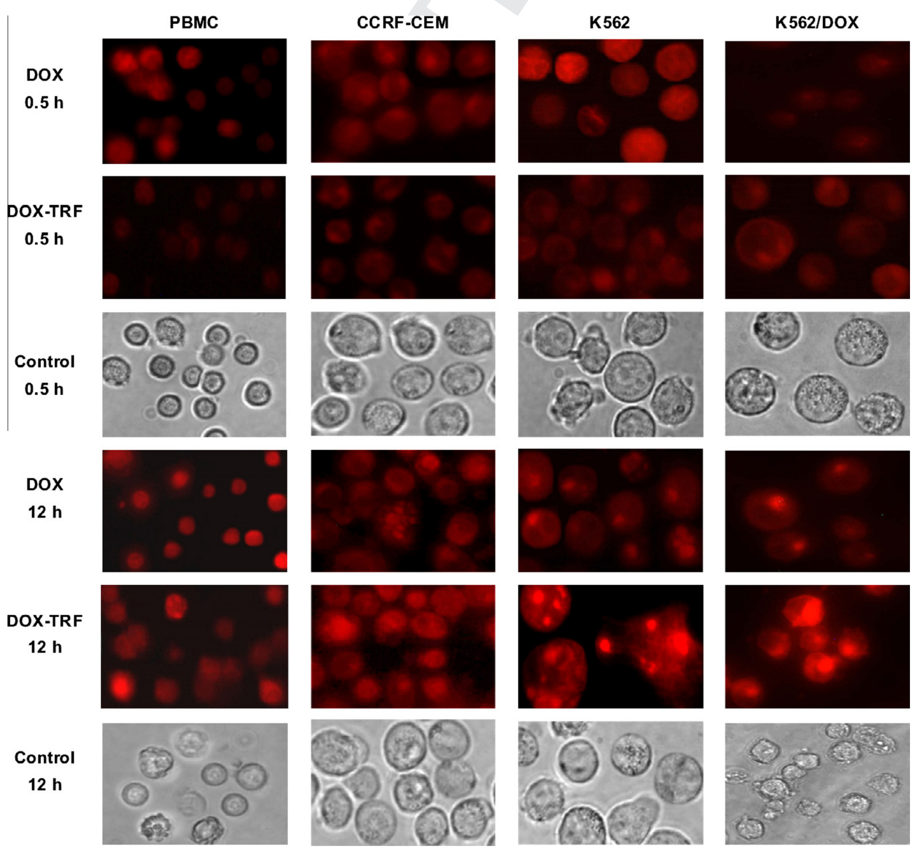

Fig. 4. Intracellular accumulation and distribution of DOX and DOX–TRF in PBMC, CCRF-CEM, K562 and K562/DOX cell lines. The cells were incubated with 0.5 μM DOX alone and conjugated to TRF for 0.5 and 12 h. The cells were monitored using an Olympus IX70, Japan; magnification 400×.

Please cite this article in press as: Szwed, M., et al. Transferrin as a drug carrier: Cytotoxicity, cellular uptake and transport kinetics of doxorubicin transferrin conjugate in the human leukemia cells. Toxicol. in Vitro (2013), http://dx.doi.org/10.1016/j.tiv.2013.09.013

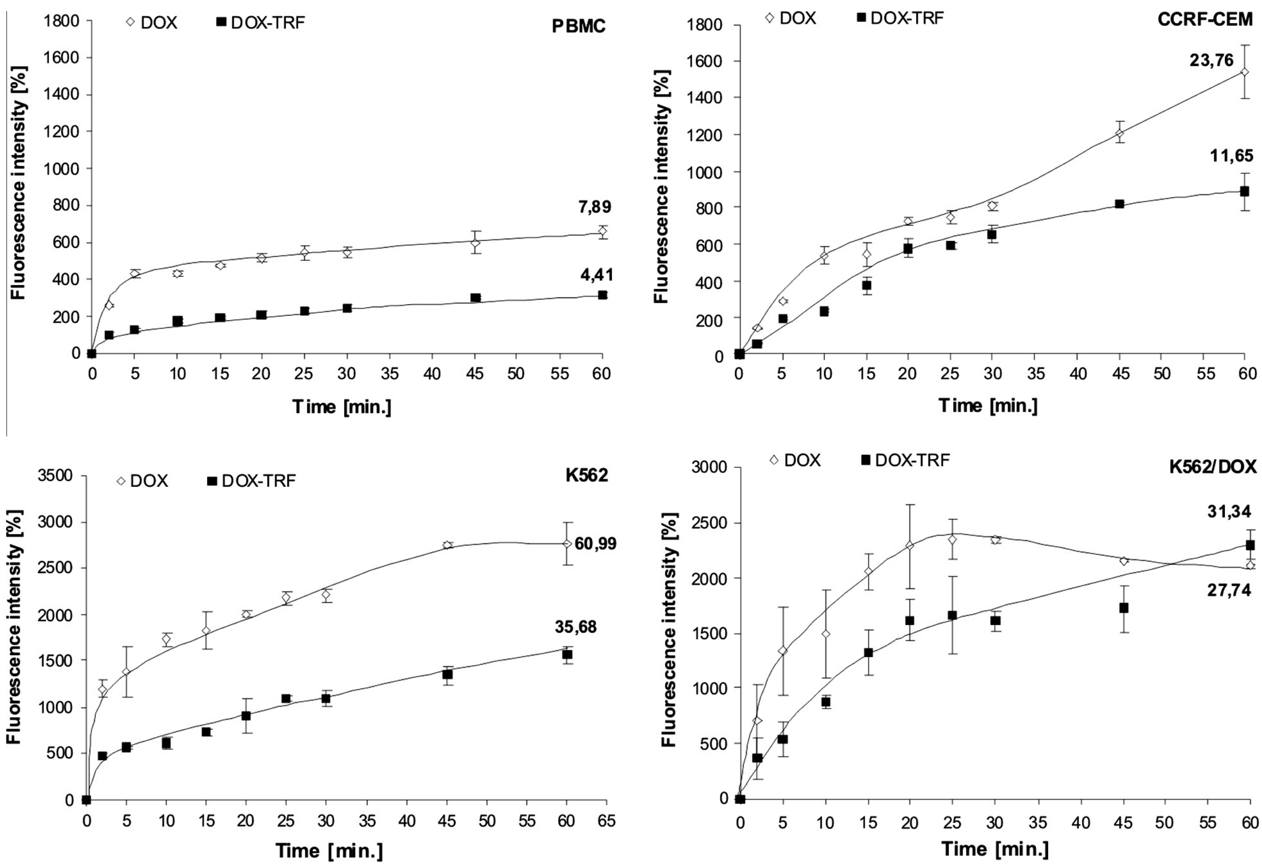

Fig. 5. Uptake of DOX or DOX–TRF by PBMC, CCRF-CEM, K562, K562/DOX cells in the function of time. Moreover, flow cytometry analysis allowed the evaluation of the values of direction components, which are the measurement of the drug influx to the cell. The results are the means ± SD of 3–4 independent experiments. In each line as in PBMC we observed a significant difference between transport of free DOX and DOX–TRF.

4. Discussion

Tumor-targeted delivery of anticancer drugs appears to be one of the most important ways to improve cancer chemotherapy (Liu et al., 2010; Maeda et al., 2009). Macromolecular drug carriers have been shown to be effective in overcoming many obstacles of conventional chemotherapy. A macromolecular drug carrier can easily enter the tumors and enhance drug accumulation due to vascular leakiness and important lymphatic drainage in cancers (Moon et al., 2007). The studies carried out on rat models have shown that human recombinant melanotransferrin (p97), covalently linked with paclitaxel (PTX) and DOX, could be actively transported across the Blood–Brain–Barrier (BBB) and its accumulation in an *in vitro* model was 10–15 times higher than the combination of free drugs (Karkan et al., 2008).

The knowledge about the structure of proteins which can be used as drug carriers for rational drug design is still very limited. This is due to the poor suitability of classical methods of structural analysis for the investigation of homogenous peptides or proteins. MS is currently the most accurate analytical method with a wide variety of applications for the analysis of physicochemical properties of potential drug carriers (Kloniecki et al., 2011). It allows the evaluation of three parameters characterizing given ion beams: the ion mass and the individual ion's contents and energy. We assessed by this method that one molecule of protein can bind two molecules of drug.

These results allowed us to carry out ion mobility separation measurements, also used to characterize Aβ peptides in Alzheimer's disease (Cappai and Barnham, 2008; Kokubo et al., 2005). IMS provided a simple and fast insight into the shape of DOX–TRF conjugate allowing the testing of changes in the structure of transferrin after drug binding. Drift times measurements led to the conclusion that the structure of TRF after doxorubicin binding did not change, because there was no difference between the collisional cross sections for TRF and DOX–TRF.

The conjugation of DOX to TRF greatly enhanced DOX cytotoxicity in leukemic cells. This was the reverse in PBMC, which were more resistant to the conjugate than to DOX alone. Chlorambucil-TRF conjugates were also shown to be effective in cancer therapy. This formulation was active against the breast cancer cell line MCF-7 and the leukemia cell line MOLT4 with a decrease in chlorambucil IC_{50} parameter of about 18-fold. Studies in mice have confirmed that this formulation of chlorambucil is much better incorporated by tumor cells than free drug (Beyer et al., 1998). Similarly, a cisplatin–transferrin conjugate presented a much higher cytotoxicity than the free drug. Inuma et al. (2002) reported that it increased significantly the lifespan of mice bearing the MKN45P gastric cancer.

In addition, DOX–TRF conjugates may overrun the multidrug resistance barrier which limits the success of cancer therapies. Lubgan et al. (2009) showed that DOX–TRF is about 300 times more cytotoxic than doxorubicin to the doxorubicin-resistant HL60 cell line. DOX-antibody conjugates may also be worthy of interest. Starting from the fact that the midkine receptor is a growth factor receptor preferentially expressed in tumor cells, Inoh et al. (2006) studied an anti-midkine receptor – doxorubicin conjugate. However, this immunoconjugate did not inhibit the growth of HepG2 cells.

Many authors suggest that transferrin, which is used in the conjugate as a drug carrier, binds to the TRF receptor and enters the

Please cite this article in press as: Szwed, M., et al. Transferrin as a drug carrier: Cytotoxicity, cellular uptake and transport kinetics of doxorubicin transferrin conjugate in the human leukemia cells. Toxicol. in Vitro (2013), http://dx.doi.org/10.1016/j.tiv.2013.09.013

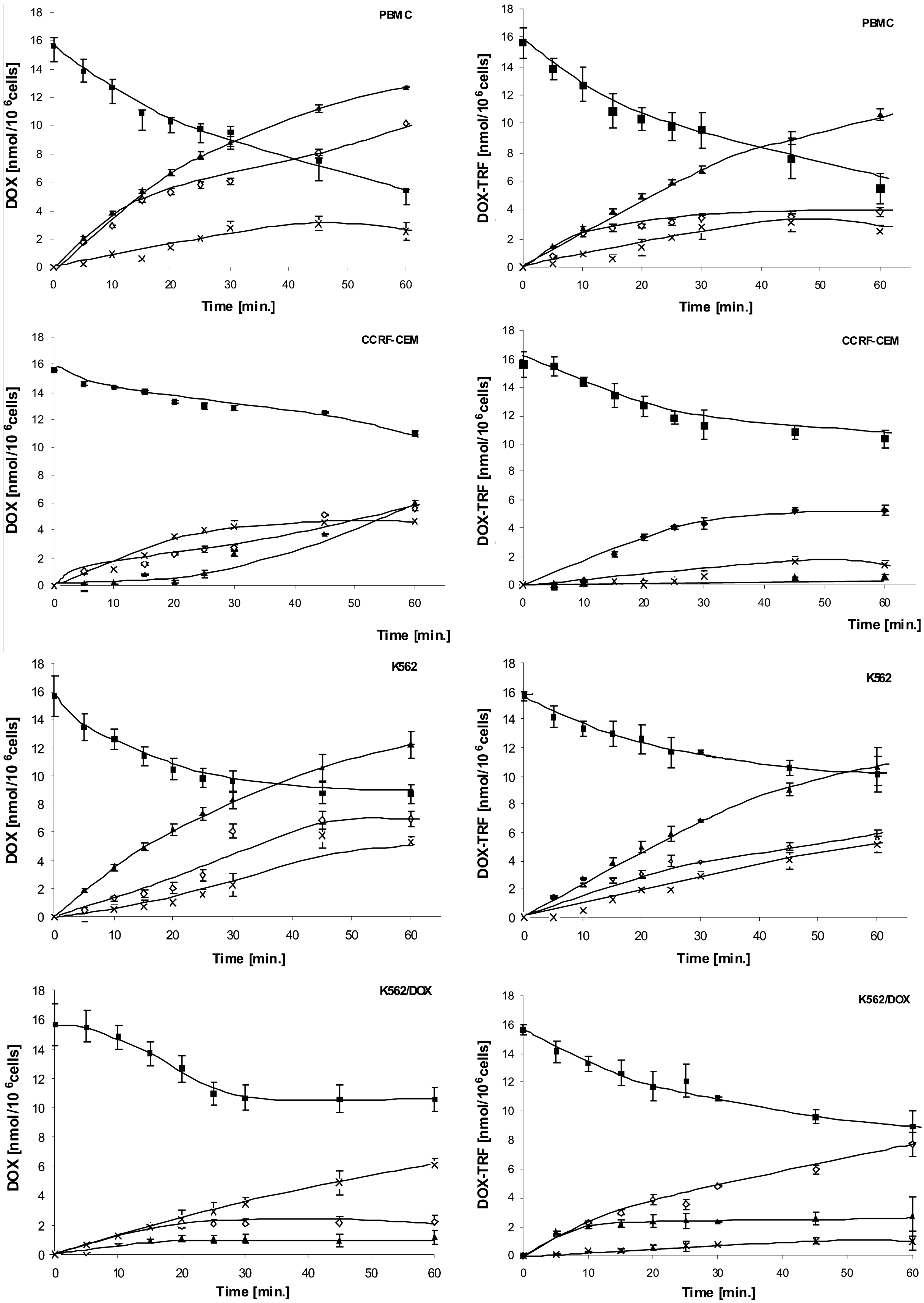

Fig. 6. Drug uptake (▲) and efflux (x) by lymphocytes and leukemic cell lines. (■): Amount of drug in external medium; (◇): amount of cell-associated drug. Data are the means ± SD of six independent experiments.

Table 3
The comparison of transport parameters for PBMC, CCRF-CEM, K562 and K562/DOX cells treated with DOX or DOX–TRF. k_{in}—influx rate constant; V_{in}—influx rate; $U_{t=60}$—drug taken up by cells within 60 min; k_{out}—efflux rate constant; V_{out}—efflux rate, $E_{t=60}$—drug removed by cells within 60 min. Results represent means ± SD of six independent experiments. Statistical analysis was performed by using Tukey's test and the significance level was assumed as $\alpha \leqslant 0.05$. We compared the differences for DOX transport and DOX–TRF within the same cell line (bold text), the differences between normal and leukemic cells in the transport of DOX (*) or DOX–TRF($^{\#}$), respectively. Moreover, we also analyzed the differences in the transport of DOX (single underline) and DOX–TRF conjugate (double underline) between K562 cells sensitive and resistant to DOX.

Parameters	Peripheral blood mononuclear cells		CCRF-CEM		K562		K562/DOX	
	DOX	**DOX–TRF**	DOX	DOX–TRF	DOX	DOX–TRF	DOX	DOX-TRF
Cells								
k_{in} (min^{-1})	**0.028 ± 0.005**	**0.019 ± 0.001**	0.012 ± 0.001*	0.008 ± 0.002$^{\#}$	**0.025 ± 0.002**	**0.019 ± 0.001**	0.008 ± 0.00041	0.021 ± 0.0014
V_{in} (nmol/min)	**0.442 ± 0.044**	**0.301 ± 0.024**	0.171 ± 0.01*	0.126 ± 0.008$^{\#}$	**0.395 ± 0.012**	**0.297 ± 0.023**	0.131 ± 0.002	0.330 ± 0.011
$U_{t=60}$ (nmol/min/10^{6} cells)	**10.179 ± 0.244**	**3.409 ± 0.347**	5.276 ± 0.0335*	4.584 ± 0.378	**6.917 ± 0.531**	**3.504 ± 0.687**	2.260 ± 0.130	2.720 ± 0.045
k_{out} (min^{-1})	0.0006 ± 0.001	0.0015 ± 0.0002	**0.0025 ± 0.001***	**0.0010 ± 0.0003**	**0.0040 ± 0.0007**	**0.0014 ± 0.0005**	**0.0060 ± 0.0004**	**0.0007 ± 0.0001**
V_{out} (nmol/min)	0.0097 ± 0.002	0.0145 ± 0.001	**0.0437 ± 0.002***	**0.0137 ± 0.001**	**0.0715 ± 0.005**	**0.0215 ± 0.002**	**0.0937 ± 0.0009***	**0.0022 ± 0.0003**$^{\#}$
$E_{t=60}$ (nmol/min/10^{6} cells)	2.535 ± 0.410	1.535 ± 0.358	**3.355 ± 0.157***	**1.378 ± 0.293**	**3.680 ± 0.406**	**1.160 ± 0.0643**	**6.130 ± 0.400***	**1.010 ± 0.089**

cell through clathrin-mediated endocytosis. DOX–TRF conjugate, internalized into the cell, is sorted along the trafficking pathway into endosomes (Mayle et al., 2012). It is proposed that prior to doxorubicin being separated from the protein, it can be metabolized as free drug (Florent and Monneret, 2008). However, as shown by Lubgan et al. (2009), glutaraldehyde used in the conjugate as a linker between the anthracycline and TRF forms a Shiff base which makes the conjugate very stable in the cytosol. Therefore, DOX–TRF is not a substrate for endogenous human enzymes and may transform in the endosomes/lysosomes to some derivative metabolites (Kratz et al., 2008). Probably this is the reason why doxorubicin binding to TRF is observed far later in the nucleus than free drug and can cause cell death effectively. This hypothesis was confirm in the fluorescence microscopy evaluation which compares the cellular distribution of both drug formulations (Fig. 4). We have shown that the DOX conjugate was initially often located in the cytoplasm, possibly in endosomal – like related structures. The microscopic observation of normal lymphocytes during drug treatment also showed a different location of DOX and DOX–TRF, indicating that the mechanism of plasma membrane passage and subsequent intracellular routing are different between both drugs. A predominantly cytoplasmic location of DOX–TRF potentially exposes the conjugate to bioreductive processes that are known to play an important role in DOX cytotoxicity. The metabolism of free DOX takes place in the cytosol. DOX, during redox-activation to a semiquinone intermediate. can generate superoxide anion that later produces another ROS generation. ROS which is formed during these transformation can damage proteins, lipids as well as DNA. Subsequently, oxidative stress is involved in the initiation or the execution of DNA lesions and influences the formation of the oxidized DNA bases (Gewirtz, 1999; Injac and Strukelj, 2008).

Our results are in agreement with those of Kovár et al. (2007), which show differences in the morphology of EL-4T lymphoma cells exposed to free DOX or DOX conjugated to a HPMA copolymer carrier via enzymatically (PK1) degradable bonds. The fluorescence of free DOX was located mainly inside the nucleus and endosomal-like related structures, whereas the fluorescence of DOX in the PK1 conjugate was mainly found inside the nucleus and acidic organelles. In addition, a doxorubicin–HPMA conjugate bound via a pH sensitive bond (HYD) presented similar biological properties to our DOX–TRF conjugate. Controlled release of DOX from HPMA within cancer cells is likely to be achieved by hydrolysis of hydrazone conjugates (Seib et al., 2006) affecting mainly the cytoplasmic location of DOX–TRF conjugate.

Differences in intracellular drug accumulation and distribution of anticancer drugs in cancer cells may contribute to resistance to chemotherapy. We observed significant differences in the intracellular fate of the two DOX formulations. In our experiments, flow cytometry was used to evaluate intracellular anthracycline content. For short incubations, higher fluorescence intensity was observed for DOX than for DOX–TRF; that was the reverse after 12 h of incubation. Of utmost interest is the difference between cancer and normal cells. Peripheral blood mononuclear cells were less sensitive than leukemia cells to DOX–TRF, although both drugs were removed similarly by cells over 60 min. Ren and Wei (2004) examined the intracellular levels of an oligodeoxynucleotide–doxorubicin conjugate in human epidermoid carcinoma and suggested that there are two separate phases in conjugate uptake: a rapid initial uptake during the first 8 h of incubation followed by a small increase of drug fluorescence until the end of incubation.

Sensitivity of cancer cells to anticancer agents is enabled by the presence of constant intra- and extracellular drug concentrations. An important factor is therefore the clearance of the drug (Chen et al., 2006). Differences in cytotoxicity between free DOX and DOX–TRF may reflect, at least in part, differences in the mechanism of intracellular uptake of drugs and time-dependent distribution. We examined the relative contribution of uptake and efflux of DOX–TRF in the different cell types in order to determine transport kinetic parameters. DOX uptake was faster than that of DOX–TRF.

The comparison of the kinetic parameters revealed that the quantity of free DOX taken up by cells within 60 min of incubation was greater for normal than for cancer cells, whereas no difference in intracellular DOX–TRF distribution was observed in cancer and normal cells. Furthermore, the influx and efflux rate constants, as well as initial influx and efflux rates showed that the kinetics of drug transport was different for DOX and DOX–TRF. This is in agreement with the study of Wu et al. (2007) who showed that free DOX and DOX bound to a macromolecular carrier have very different kinetic properties, both in terms of *in vitro* cellular uptake and *in vivo* plasma residence time. To improve drug tumor accumulation, liposomes co-encapsulating doxorubicin and verapamil were conjugated to transferrin to provide a mechanism for tumor cell – selective targeting (Wu et al., 2007). Encapsulating the drug in liposomes allows the delivery of the drug into the cells interior through vascular fusion with the membrane rather than passive diffusion of the drug across the membrane. These authors observed that DOX cellular uptake of TRF–DOX/VER was actually lower than that of DOX–VER over 72 h. This suggests that the mechanism of cellular entry (receptor mediated endocytosis for TRF liposomes versus passive diffusion for free drug) is an important determinant for cytotoxicity. Similarly, a higher amount of doxorubicin uptake was also observed in CCRF-CEM cells incubated with a DOX conjugate obtained by covalent linkage to the DNA aptamer sgc8c (Huang et al., 2007). It was found that other nanoparticles, aptamers used as drug carriers led to improved DOX transport to cancer cells (Chang et al., 2011; Donovan et al., 2011).

In summary, the data presented in the paper suggest that the cellular mechanism of anti-proliferative action of DOX–TRF is different than that of free DOX. Leukemic cells and normal ones have different trafficking pathways and levels of enzymes able to cleave DOX from its carrier. Besides this, the cellular accumulation of the conjugate is dependent on a dynamic balance between influx and efflux processes. In addition, active transport mechanisms can mediate intracellular drug sequestration, rendering possible the intracellular unbinding of the drug from its carrier.

Binding low molecular weight anticancer therapeutics to macromolecular carriers may give several advantages, such as improved solubility, biodistribution and pharmacokinetic profiles. Transferrin conjugates may improve doxorubicin use in many different ways. We have shown that different mechanisms of transport are operative for free doxorubicin and DOX–TRF malignant cells were able to retain the conjugate for longer periods of time than normal lymphocytes. We observed limited effects of the conjugate on normal cells, which did not over-express the transferrin receptor. Differences in cytotoxicity and accumulation levels of DOX–TRF and DOX warrants further development of this formulation.

Conflict of interest

Q3 The authors declare no conflict of interest.

Acknowledgements

We thank Prof. G. Bartosz for making available CCRF-CEM cells. This work was supported by the European Union from the European Social Fund and the state budget within the Integrated Regional Operational Program and by Ministry of Science and Higher Education grant N N405 161439.

References

Andreoni, A., Colasanti, A., Colasanti, P., Kisslinger, A., Mastrocinque, M., Riccio, P., Roberti, G., 1996. Kinetic transport analysis of daunorubicin by LoVo and LoVo/DX cells. Photochem. Photobiol. 64, 159–162.
Barabas, K., Sizensky, J.A., Faulk, W.P., 1992. Transferrin conjugates of adriamycin are cytotoxic without intercalating nuclear DNA. J. Biol. Chem. 5, 9437–9442.
Berczi, A., Ruthner, M., Szuts, V., Fritzer, M., Schweizner, E., Goldenberg, H., 1993. Influence of conjugation of doxorubicin to transferrin on the iron uptake by K562 cells via receptor-mediated endocytosis. Eur. J. Biochem. 213, 427–436.
Beyer, U., Roth, T., Schumacher, P., Maier, G., Unold, A., Frahm, A.W., Fiebig, H.H., Unger, C., Kratz, F., 1998. Synthesis and in vitro efficacy of transferrin conjugates of the anticancer drug chlorambucil. J. Med. Chem. 41, 2701–2708.
Cappai, R., Barnham, K.J., 2008. Delineating the mechanism of Alzheimer's disease Aβ peptide neurotoxicity. Neurochem. Res. 33, 526–532.
Chang, M., Yang, C.S., Huang, D.M., 2011. Aptamer-conjugated DNA icosahedral nanoparticles as a carrier of doxorubicin for cancer therapy. ACS Nano 23, 6156–6163.
Chen, V.Y., Posada, M.M., Blazer, L.L., Zhao, T., Rosania, G.R., 2006. The role of the VPS4A-exosome pathway in the intrinsic egress route of a DNA-binding anticancer drug. Pharm. Res. 23, 1687–1695.
Donovan, M.J., Meng, L., Chen, T., Zhang, Y., Sefah, K., Tan, W., 2011. Aptamer-drug conjugation for targeted tumor cell therapy. Method Mol. Biol. 764, 141–152.
Florent, J.C., Monneret, C., 2008. Doxorubicin conjugates for selective delivery to tumors. Top. Curr. Chem. 283, 99–140.
Gewirtz, D.A., 1999. A critical evaluation of the mechanisms of action proposed for the antitumor effects of the anthracycline antibiotics adriamycin and daunorubicin. Biochem. Pharmacol. 7, 727–741.
Giles, K., Pringle, S.D., Worthington, Little, D., Wildgoose, J.L., Bateman, R.H., 2004. Applications of a travelling wave-based radio-frequency-only stacked ring ion guide. Rapid Commun. Mass Spectrom. 18, 2401–2414.
Haag, R., Kratz, F., 2006. Polymer therapeutics: concepts and applications. Angew. Chem. Int. Ed. Engl. 45, 1198–1215.
Huang, G., Mills, L., Worth, L.L., 2007. Expression of human glutathione S-transferase P1 mediates the chemosensitivity of osteosarcoma cells. Mol. Cancer Ther. 6, 1610–1619.
Injac, R., Strukelj, B., 2008. Recent advances in protection against doxorubicin-induced toxicity. Technol. Cancer Res. Treat. 7, 497–516.
Inoh, K., Muramatsu, H., Torii, S., Oda, M., Kumai, H., Sakuma, S., Inui, T., Kimura, T., Muramatsu, T., 2006. Doxorubicin-conjugated anti-midkine monoclonal antibody as a potential anti-tumor drug. Jpn. J. Clin. Oncol. 36, 207–211.
Inuma, H., Maruyama, K., Okinawa, K., Sasaki, K., Sekine, T., Ishida, O., Ogiwara, N., Johkura, K., Yonemura, Y., 2002. Intracellular targeting therapy of cisplatin-encapsulated transferrin-polyethyleneglycol liposome on peritoneal dissemination of gastric cancer. Int. J. Cancer 99, 130–137.
Jungsuwadee, P., Zhao, T., Stolarczyk, E.I., Paumi, C.M., Butterfield, D.A., St Clair, D.K., Vore, M., 2012. The G671V variant of MRP1/ABCC1 links doxorubicin-induced acute cardiac toxicity to disposition of the glutathione conjugate of 4-hydroxy-2-trans-nonenal. Pharmacogenet. Genomics 22, 273–284.
Karkan, D., Pfeifer, C., Vitalis, T.Z., Arthur, G., Ujiie, M., Chen, Q., Tsai, S., Koliatis, G., Gabathuler, R., Jefferies, W.A., 2008. A unique carrier for delivery of therapeutic compounds beyond the blood-brain barrier. PLoS ONE 25. http://dx.doi.org/10.1371/journal.pone.0002469.
Kloniecki, M., Jablonowska, A., Poznanski, J., Langridge, J., Hughes, C., Campuzano, I., Giles, K., Dadlez, M., 2011. Ion mobility separation coupled with MS detects two structural states of Alzheimer's disease Aβ1-40 peptide oligomers. J. Mol. Biol. 4071, 110–124.
Kokubo, H., Kayed, R., Glabe, C.G., Yamaguchi, H., 2005. Soluble Aβ oligomers ultrastructurally localize to cell processes and might be related to synaptic dysfunction in Alzheimer's disease brain. Brain Res. 1031, 222–228.
Kovár, L., Strohalm, J., Chytil, P., Mrkvan, T., Kovár, M., Hovorka, O., Ulbrich, K., Říhová, B., 2007. The same drug but a different mechanism of action: comparison of free doxorubicin with two different N-(2 hydroxypropyl)methacrylamide copolymer-bound doxorubicin conjugates in EL-4 cancer cell line. Bioconjug. Chem. 1, 894–902.
Kratz, F., Muller, I.A., Ryppa, C., Warnecke, A., 2008. Prodrug strategies in anticancer chemotherapy. Chem. Med. Chem. 3, 20–53.
Liu, Y.H., Di, Y.M., Zhou, Z.W., Mo, S.L., Zhou, S.F., 2010. Multidrug resistance-associated proteins and implications in drug development. Clin. Exp. Pharmacol. Physiol. 37, 115–120.
Lubgan, D., Marczak, A., Distel, L., Jóźwiak, Z., 2006. Transferrin conjugates in the anticancer therapy. Postepy Biochem. 52, 72–79.
Lubgan, D., Jóźwiak, Z., Grabenbauer, G.G., Distel, L., 2009. Doxorubicin–transferrin conjugate selectively overcomes multidrug resistance in leukaemia cells. Cell. Mol. Biol. Lett. 1, 113–127.
Luo, Y.L., Shiao, Y.S., Huang, Y.F., 2011. Release of photoactivatable drugs from plasmonic nanoparticles for targeted cancer therapy. ACS Nano 25, 7796–7804.
Maeda, H., Bharate, G.Y., Daruwalla, J., 2009. Polymeric drugs for efficient tumor-targeted drug delivery based on EPR-effect. Eur. J. Pharm. Biopharm. 71, 409–419.
Mayle, K.M., Le, A.M., Kamei, D.T., 2012. The intracellular trafficking pathway of transferring. Biochim. Biophys. Acta 1820, 264–281.
Moon, C., Kwon, Y.M., Lee, W.K., Park, Y.J., Yang, V.C., 2007. Yang, in vitro assessment of a novel polyrotaxane-based drug delivery system integrated with a cell-penetrating peptide. J. Control. Release 4, 43–50.
Myung, S., Lee, Y.J., Moon, M.H., Taraszka, J., Sowell, R., Koeniger, S., 2003. Development of high-sensitivity ion trap ion mobility spectrometry time-of-flight techniques: a high-through put nano-LC-IMS-TOF separation of peptides arising from a Drosophila protein extract. Anal. Chem. 75, 5137–5145.
Nevozhay, D., Kanska, U., Budzynska, R., Boratynski, J., 2007. Current status of research on conjugates and related drug delivery systems in the treatment of cancer and other diseases. Postepy. Hig. Med. Dosw. 61, 350–360.
Przybylska, M., Koceva-Chyla, A., Rozga, B., Jozwiak, Z., 2001. Cytotoxicity of daunorubicin in trisomic (+21) human fibroblasts: relation to drug uptake and cell membrane fluidity. Cell Biol. Int. 25, 157–170.
Ren, Y., Wei, D., 2004. Quantification intracellular levels of oligodeoxynucleotide–doxorubicin conjugate in human carcinoma cells in situ. J. Pharm. Biomed. Anal. 29, 387–391.
Ruotolo, B.T., Hyung, S.J., Robinson, P.M., Giles, K., Bateman, R.H., Robinson, C.V., 2007. Ion mobility mass spectrometry reveals long-lived, unfolded intermediates in the dissociation of protein complexes. Angew. Chem. Int. Ed. Engl. 46, 8001–8004.
Ruotolo, B.T., Benesch, J.L., Sandercock, A.M., Hyung, S.J., Robinson, C.V., 2008. Ion mobility mass spectrometry analysis of large protein complexes. Nat. Protoc. 3, 1139–1152.
Salvatorelli, E., Menna, P., Surapaneni, S., Aukerman, S.L., Chello, M., Covino, E., Sung, V., Minotti, G., 2012. Pharmacokinetic characterization of amrubicin cardiac safety in an ex vivo human myocardial strip model I. Amrubicin accumulates to

a lower level than doxorubicin or epirubicin. J. Pharmacol. Exp. Ther. 15, 464–473.

Seib, F.P., Jones, A.T., Duncan, R., 2006. Establishment of subcellular fractionation techniques to monitor the intracellular fate of polymer therapeutics I. Differential centrifugation fractionation B16F10 cells and use to study the intracellular fate of HPMA copolymer – doxorubicin. J. Drug Target. 14, 375–390.

Swiech, O., Mieczkowska, A., Chmurski, K., Bilewicz, R., 2012. Intermolecular Interactions between doxorubicin and β-cyclodextrin 4-methoxyphenol conjugates. J. Phys. Chem. B 16, 1765–1771.

Tanaka, T., Fujishima, Y., Kaneo, Y., 2001. Receptor mediated endocytosis and cytotoxicity of transferrin–mitomycin C conjugate in the HepG2 cell and primary cultured rat hepatocyte. Biol. Pharm. Bull. 24, 268–273.

Tsuruo, T., Iida-Saito, H., Kawabata, H., Oh-hara, T., Hamada, H., Utakoji, T., 1986. Characteristics of resistance to adriamycin in human myelogenous leukemia K562 resistant to adriamycin and in isolated clones. Jpn. J. Cancer Res. 7, 682–692.

Wu, J., Lu, Y., Lee, A., Pan, X., Yang, X., Zhao, X., Lee, R.J., 2007. Reversal of multidrug resistance by transferrin-conjugated liposomes co-encapsulating doxorubicin and verapamil. J. Pharm. Pharm. Sci. 10, 350–357.

Please cite this article in press as: Szwed, M., et al. Transferrin as a drug carrier: Cytotoxicity, cellular uptake and transport kinetics of doxorubicin transferrin conjugate in the human leukemia cells. Toxicol. in Vitro (2013), http://dx.doi.org/10.1016/j.tiv.2013.09.013